

Highly Microporous Activated Carbon from Acorn Nutshells and its Performance in Water Vapor Adsorption

Chairunnisa

Department of Energy and Environmental Engineering, Interdisciplinary Graduate School of Engineering Sciences, Kyushu University

K. Thu

Department of Energy and Environmental Engineering, Interdisciplinary Graduate School of Engineering Sciences, Kyushu University

T. Miyazaki

Department of Energy and Environmental Engineering, Interdisciplinary Graduate School of Engineering Sciences, Kyushu University

Nakabayashi, Koji

Advanced Device Materials, Institute for Material Chemistry and Engineering, Kyushu University

他

<https://doi.org/10.5109/4372285>

出版情報 : Evergreen. 8 (1), pp.249-254, 2021-03. Transdisciplinary Research and Education Center for Green Technologies, Kyushu University

バージョン :

権利関係 : Creative Commons Attribution-NonCommercial 4.0 International



Highly Microporous Activated Carbon from Acorn Nutshells and its Performance in Water Vapor Adsorption

Chairunnisa^{1,*}, K. Thu², T. Miyazaki³, K. Nakabayashi⁴, J. Miyawaki⁵, A. T. Wijayanta⁶, F. Rahmawati⁷

^{1,2,3} Department of Energy and Environmental Engineering, IGSES, Kyushu University, Japan

^{1,2,3} International Institute for Carbon-Neutral Energy Research, Kyushu University, Japan

^{4,5} Advanced Device Materials, Institute for Material Chemistry and Engineering, Kyushu University, Japan

¹Department of Science, Sumatera Institute of Technology, Lampung, 35365, Indonesia

⁶ Department of Mechanical Engineering, Universitas Sebelas Maret, Jawa Tengah, 57126, Indonesia

⁷ Department of Chemistry, Universitas Sebelas Maret, Jawa Tengah, 57126, Indonesia

*E-mail: chairunnisa.365@s.kyushu-u.ac.jp

(Received September 24, 2020; Revised March 25, 2021; accepted March 26, 2021).

Abstract: The green preparation of microporous activated carbon using acorn nutshell with different production conditions was studied. The heating rate and nitrogen flow rate were controlled during preparation. The effect of those conditions on the surface properties and water adsorption performance was observed. According to the results, the total surface area of acorn nutshells-based activated carbon can reach up to 993 m²/g with 90% microporosity and a total pore volume of 0.49 cm³/g. The water adsorption uptake under $P/P_0 = 0.9$ of prepared material is up to 0.39 g/g. This study found that acorn nutshell shows potential performance as a precursor for producing highly microporous activated carbon, which might be suitable for water vapor adsorption.

Keywords: activated carbon; microporous; acorn nutshells; water adsorption; steam activation

1. Introduction and background

The unique physical and chemical properties of activated carbon make it an important material for various fields. Activated carbon has been primarily utilized in adsorption applications such as liquid-based^{(1),(2)} and gas adsorption^{(3),(4)}. The adsorption application by activated carbon not only for the air purification objective, but also for cooling^{(5),(6)}, dehumidification⁽⁷⁾, and even for thermal storage applications. Different methods have been developed to prepare activated carbons with various properties. Several raw materials have been used as activated carbon's precursors, such as coal^{(8),(9)}, tar⁽¹⁰⁾, and biomass waste^{(11),(12)}. Among those precursors, it is believed that biomass waste is a low-cost and green precursor, and its utilization might reduce solid waste and increase the waste's economic value.

In the production of activated carbon, the activation step is necessary to remove molecules that clogged the exhibited pores and develop them. The activation process is classified into chemical and physical activation. Chemical activation is conducted by using salts⁽¹³⁾, bases⁽³⁾, or acid⁽¹⁴⁾. Physical activation is proceeded by using some gasses such as CO₂⁽¹⁵⁾, air^{(16),(17)}, or steam^{(18),(19)}. Physical activation is an environmentally benign method compare with chemical activations due to unnecessary post-treatment such as washing, which significantly reduced

the wastewater produced from the activation step.

In this study, the activated carbon was produced from Acorn nutshell to develop biomass waste-based activated carbon with suitable properties for water vapor adsorption. It is worth noting that activated carbon naturally has an almost hydrophobic surface. However, due to the small amount of active hydrophilic functional groups available on the surface of activated carbon, this material has the ability to adsorb the water vapor⁽²⁰⁾. Compared with the commercial desiccant materials, such as silica gels and other alumina-silica materials, activated carbon has different water vapor adsorption properties, and one of the most advantages own by it is the easiness of water vapor to be desorbed from the adsorbent, which thus hopefully lowering the regeneration temperature of the material.

Microporosity plays an essential part in the ability of activated carbon for water vapor adsorption application. One way to produce activated carbon with high amounts of micropores is by physical activation, such as steam activation. It was reported before that steam can produce high microporosity of activated carbon⁽¹¹⁾. Mamani et al.⁽²¹⁾ reported that activated carbon from lingo-cellulosic biomass prepared by steam activation has 74% microporosity. Furthermore, Heo et al.⁽²²⁾ produced high microporous activated from cellulose fibers by using steam activation. Not only the number of micropores is

essential, but the size of the micropore itself should also be controlled since the adsorption of water vapor strongly depends on the size of micropore²³). Controlling the microporosity of activated carbon prepared by steam activation is challenging due to the rapid reaction between steam and the wall of carbon material. Therefore, in this study, the activated carbon using steam activation was prepared, and the microporosity of the prepared material was controlled by using different preparation conditions. Then, the performance of prepared activated carbon for water vapor adsorption was studied under different relative pressures.

2. Methodology

2.1 Materials and sample preparation

Acorn nutshell was dried at 100°C overnight and ground before carbonization. About 11 g of dried powdered-nutshell was put into an alumina crucible (placed inside the furnace equipped with temperature controller) and heated using different heating rate: 5°C/min, 10°C/min, and 15°C/min from 25°C to 900°C under different N₂ stream (100 cc/min; 200 cc/min; 400 cc/min; and 500 cc/min). The materials produced from the carbonization step were labeled as C. The C prepared from different carbonization conditions was then activated by using steam activation. The activation was conducted using the same system with different heating and N₂ flow rate. The activation was done using a temperature of 900°C for 10 minutes to avoid excess burn-off. The details of preparation conditions were presented in Table 1.

Table 1. Preparation conditions

Samples	Carbonization condition		Activation condition	
	HR (°C/min)	NR (cc/min)	HR (°C/min)	NR (cc/min)
C1	5	200	Without activation	
C2	10	200		
C3	15	200		
AC1	5	200	5	200
AC2	10	200	10	200
AC3	15	200	15	200
C4	15	100	Without activation	
C5	15	400		
C6	15	500		
AC4	15	100	15	100
AC5	15	400	15	400
AC6	15	500	15	500
AC7	5	200	15	200

*HR = heating rate, NR = N₂ flow rate, C = char, AC = activated carbon

2.2 Characterization

The % yield of C and AC was calculated after

carbonization and activation steps using the equation below:

$$\text{Yield (\%)} = \frac{\text{Carbon material mass}}{\text{Raw material mass}} \times 100\% \quad (1)$$

The thermal degradation of acorn nutshells was measured using EXSTAR TG/DTA6000, SII at 25°C to 900°C with N₂ flow rate of 200 cc/min and a heating rate of 10°C/min. The pore properties were analyzed using nitrogen adsorption-desorption at 77K (NOVA 3200e Quantachrome, USA). The samples were first degassed at 120°C for more than 5 h to remove the adsorbed gas before measurement. The obtained N₂ adsorption isotherms were used to analyze the pore properties of activated carbon. DFT method provided by Quantachrome was utilized to determine the total surface area (A_{tot}), micropore surface area (S_{mi}), total pore volume (V_{tot}), and micropore volume (V_{mic}) of carbon materials.

The water vapor uptake of activated carbons was measured by a magnetic suspension adsorption unit of type MSB-VG-S2 supplied by Belsorp Japan, Inc at 30°C. The weight measurement resolution is 10 µg with a relative error of ±0.002% of reading. Julabo thermal stability is ±0.01°C, and fluid density accuracy is ±0.02 kg/m³. Before the measurements, the materials were degassed at 120°C for ≥ 5 h *in vacuo* (<0.133 Pa). Adsorption-desorption tests were conducted continuously. The pressure of water vapor was controlled by setting different temperatures of the vapor source. The adsorption pressure was from 0.6 kPa to 3.7 kPa, while the desorption was from 3.7 kPa to 0.6 kPa.

3. Results and Discussion

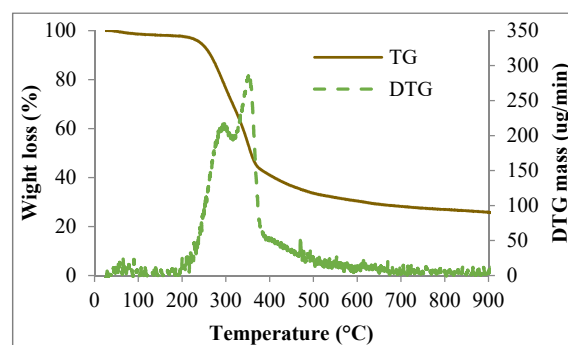


Fig. 1: TGA curve of raw material (TG = Thermogravimetry; DTG = Derivative Thermogravimetry)

The study of thermal degradation of raw material is essential as a preliminary study before selecting activated carbon precursors and deciding the preparation conditions. From Fig. 1, there is a slow rate of mass loss in the temperature range up to 200°C, which is due to the release of moisture. The mass loss in the temperature range up to 200°C to 500°C may be caused by the degradation of cellulose, hemicellulose, and lignin into a smaller organic compound and released during heating treatment²⁴). The mass loss then became lower when the temperature

increased up to 900°C, which might occur due to the hardness and complexness of the lignin structure to be degraded.

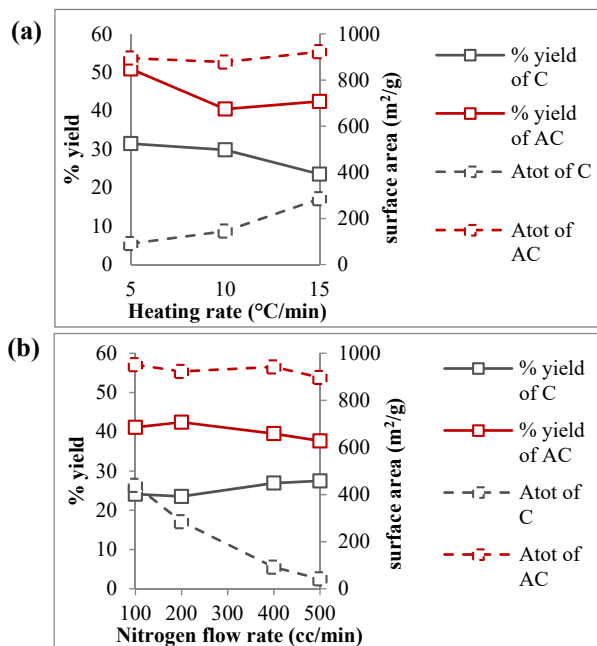


Fig. 2: The effect of heating rate (a) and nitrogen flow rate (b) on the % yield and Atot of carbon materials.

The effect of heating rate and nitrogen flow rate on the % yield and surface area of carbon materials was shown in Fig. 2. In general, it can be observed that there is an opposite relationship between the % yield and total surface area. The preparation process, which produced a low % yield, generates the carbon material with a higher total surface area.

According to Fig. 2a, the faster the heating rate used for carbonization and activation, the lower % yield of the material produced. It was reported that a faster heating rate degrades more organic molecules into tar and light gases^{25,26}, which was indicated by the decrease of % carbonization yield. The faster heating rate during carbonization also increased the A_{tot} of produced chars. For activation, a heating rate of 5°C/min produced AC with the highest % yield. The % yield decreased when 10°C/min was used and raised again when 15°C/min was utilized for activation.

On the other hand, Fig. 2b shows the relationship between N₂ flow rate with % yield and A_{tot} of carbon materials produced with the same heating rate (15°C/min). In this study, N₂ gas was used to keep the inert atmosphere in pyrolysis²⁷ and as a sweep gas to remove the char surface's volatile product and reduce the secondary reaction such as re-polymerization and recondensation²⁸. For that reason, during carbonization (pyrolysis), the higher the N₂ flow rate used, the bigger % yield of char was obtained. Different N₂ flow rates gave different tendencies on the activation step. The 200 cc/min of nitrogen flow rate resulted in AC with the biggest % yield

while the flow rate more than that, resulting in a lower % yield. The effect of N₂ flow rate on the surface area of AC also different with C. AC produced by 100cc/min and 400cc/min of N₂ flow rate shows the ACs with the highest surface area.

The effect of preparation conditions on activated carbons' porosity was reflected on the N₂ adsorption at 77 K in Fig. 3. The N₂ adsorption on acorn nutshell-based chars and activated carbon follows type I of the IUPAC classification with hysteresis type H4, which is characteristics of microporous material with slit-like pores²⁹. Fig. 3a represents the effect of heating rate while Fig. 3b shows the effect of N₂ flow rate on the porosity of chars and activated carbons. Based on the N₂ sorption uptakes on each material, it can be observed that more N₂ adsorbed on activated carbons than chars which can be assumed that activated carbon contains more pores than char. The big carbon molecules were degraded during carbonization, producing tar, releasing some volatile compounds and gasses. On the other hand, activation is the process when the tarry products that clogged the pores of char were removed by the reaction between them and the activating agent (steam) under high temperature, reducing the mass of materials, creating the new pores, and enlarging the existed pores. Thus, the carbon materials that have lower mass (% yield) possess a bigger surface area.

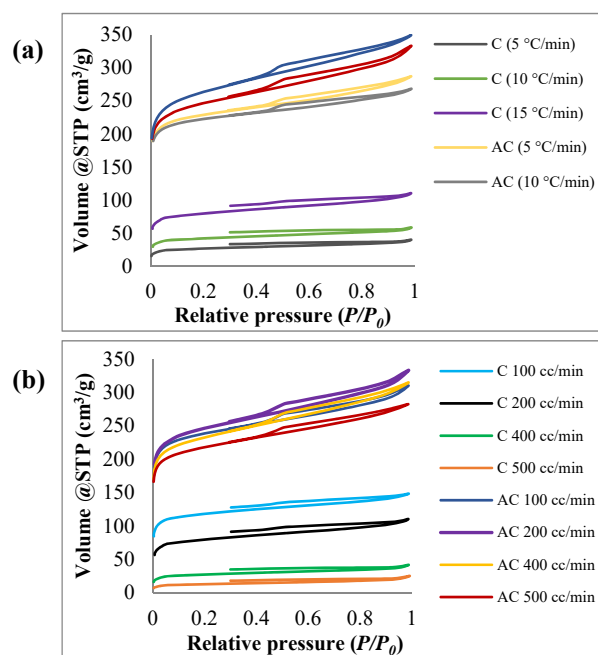


Fig. 3: N₂ adsorption isotherm on biochar and activated carbon prepared by different (a) heating rate, (b) N₂ gas flow rate

Table 2. Pore properties of Acorn nutshells based carbon materials

Samples	Pore Properties				
	A_{tot} (m^2/g)	A_{mic} (m^2/g)	V_{tot} (cm^3/g)	V_{mic} (cm^3/g)	$V_{\text{mic}}/V_{\text{tot}}$ (%)
C1	91	90	0.05	0.05	100
C2	145	145	0.08	0.07	88
C3	285	281	0.18	0.14	78
AC1	895	885	0.40	0.36	90
AC2	878	871	0.37	0.35	95
AC3	923	881	0.89	0.38	43
C4	439	436	0.20	0.19	95
C5	92	92	0.05	0.05	100
C6	42	41	0.03	0.03	97
AC4	952	939	0.43	0.38	88
AC5	942	905	0.77	0.37	48
AC6	897	885	0.40	0.36	89
AC7	993	979	0.49	0.44	90

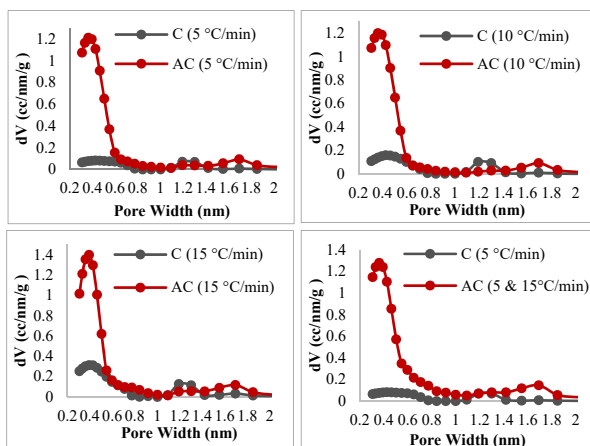


Fig. 4: Pore size distribution of acorn nutshells based carbon materials

The resume of pore properties of each material that was produced using different preparation conditions was presented in Table 2. Based on N_2 adsorption on Fig. 3 and Table 2, char that produced by 100 (C4), 200 (C3), 400 (C5), and 500 cc/min (C6) of N_2 flow rate has A_{tot} of 439 m^2/g , 285 m^2/g , 92 m^2/g , 42 m^2/g , respectively. From here, it can be claimed that the higher the N_2 flow rate utilized for carbonization, the lower the surface area of char was produced. For activation, the tendency is slightly different. The highest surface area of activated carbon was obtained when using N_2 flow rate of 200 cc/min with 5 $^\circ\text{C}/\text{min}$ of heating rate on carbonization followed by 15 $^\circ\text{C}/\text{min}$ of heating rate on activation.

Activated carbon is known for the heterogeneity of its pore size, which is classified into micropores (<2 nm), mesopores (2 nm – 50 nm), and macropores (>50 nm). From the pore size distributions in Fig. 4, the chars (C) has different size of pores. After activation (AC), more micropores with a width below 0.8 nm were produced,

which confirmed that the steam activation has the ability to produce activated carbon with high microporosity in a short duration.

In order to estimate the possible application of the synthesized activated carbons in the water vapor adsorption-based application, the adsorption isotherms of water vapor on the surface of activated carbon at 30 $^\circ\text{C}$ on prepared activated carbons were measured. Activated carbon that has been used for this adsorption study are AC3, AC4, AC7, which have the highest V_{mic} among other prepared carbon materials. Figure 5 represents the adsorption-desorption isotherm on the carbon materials with full dots are for adsorption while empty dots are for desorption.

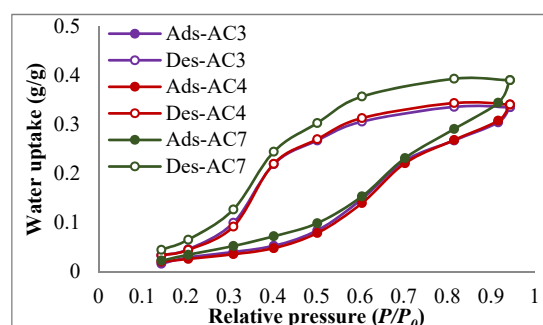


Fig. 5: Adsorption isotherm of water vapor onto activated carbons

According to Fig 5, the adsorption isotherms of water vapor onto activated carbon increases with relative pressure (P/P_0). The water adsorption on AC3, AC4, and AC7 has type V isotherm, strongly related to the adsorption of water vapor on slightly hydrophilic materials like activated carbon³⁰. Based on Fig. 5, it can be noticed that there is a steep water vapor adsorption isotherm on $P/P_0 = 0.4$ to $P/P_0 = 0.7$, which is associated with water clusters arrangement, leading to the micropore filling³¹.

According to previous research, water vapors' adsorption on activated carbons occurs only by a physical process with weak interaction between the surface of activated carbon and water vapor. The adsorption is started by the hydrogen bonding formation between available hydrophilic functional groups of activated carbon and water molecules. These attached water molecules then perform as the center of adsorption for the next coming water vapor. The water molecules then form clusters through hydrogen bonding between water-water molecules, and the clusters are located around the primary adsorption centers. At higher P/P_0 , the clusters form bridges across the pores, and when the space between clusters is too close, the increasing vapor pressure leading to the pore filling^{31,32}.

In this study, the amount of water vapor adsorbed onto AC3, AC4, and AC7 at P/P_0 0.9 were 0.33 g/g, 0.34 g/g, and 0.39 g/g, respectively. Water uptake on AC3 was close with AC4 due to their similar characteristics. Only

different N_2 flow rates were used during carbonization and activation, AC3 using 200 N_2 /min and AC4 using 100 N_2 /min. Both processes produced similar % yield and total surface area, resulting in similar water adsorption uptake. The adsorption value near saturation pressure ($P/P_0 = 0.9$) showed a strong relationship between the amounts of water uptake with V_{mic} of AC3, AC4, and AC7, which are 0.38 cm^3/g , 0.38 cm^3/g , and 0.44 cm^3/g , respectively. Therefore, it is assumed that the water adsorption mechanism on acorn nutshells-based activated carbon is strongly related to the micropore filling mechanism³³.

Based on the water vapor adsorption behavior on acorn nutshell-based-activated carbon, it can be assumed that those materials might have promising performance in removing water vapor at the range of $P/P_0 = 0.7$ to 1. Therefore, those prepared materials may be suitable to process inlet air with high humidity, such as agricultural products storage³⁴ or dehumidification systems in summer and humid places.

4 Conclusion

Different heating and nitrogen flow rate effects on activated carbon's physical properties were investigated in this work. According to the results, the heating and the nitrogen flow rate strongly affected the physical properties of the materials. It is found that the surface area of produced activated carbon was from 878 m^2/g to 993 m^2/g with a micropore volume range from 0.3 cm^3/g to 0.4 cm^3/g . The water adsorption capacity of represented material was also measured using $P/P_0 = 0.1$ to $P/P_0 = 0.9$. Based on the water sorption data, the materials' water uptake reaches the maximum value at near saturation pressure. The maximum water vapor adsorption amount onto AC3, AC4, and AC7 at 30°C were 0.33 g/g, 0.34 g/g, and 0.39 g/g, respectively, making these three materials may suitable for the removal of water vapor under high humidity condition.

Acknowledgments

The study was supported by JSPS Bilateral Programs Joint Research Projects (DG-RSTHE, Indonesia).

References

- 1) M.U. Dural, L. Cavas, S.K. Papageorgiou, and F.K. Katsaros, "Methylene blue adsorption on activated carbon prepared from *Posidonia oceanica* (L.) dead leaves: kinetics and equilibrium studies," *Chem. Eng. J.*, **168** (1) 77–85 (2011). doi:10.1016/j.cej.2010.12.038.
- 2) J. Miyawaki, J. Yeh, H.S. Kil, J.K. Lee, K. Nakabayashi, I. Mochida, and S.H. Yoon, "Influence of pore size and surface functionality of activated carbons on adsorption behaviors of indole and amylase," *Evergreen*, **3** (2) 17–24 (2016). doi:10.5109/1800868.
- 3) Y. Guangzhi, Y. Jinyu, Y. Yuhua, T. Zhihong, Y. DengGuang, and Y. Junhe, "Preparation and co₂ adsorption properties of porous carbon from camphor leaves by hydrothermal carbonization and sequential potassium hydroxide activation," *RSC Adv.*, **7** (7) 4152–4160 (2017). doi:10.1039/C6RA25303B.
- 4) M. Muttakin, A. Pal, K. Uddin, K. Thu, K. Ito, and B. Baran Saha, "Experimental study of co₂ adsorption kinetics onto activated carbon experimental study of co₂ adsorption kinetics onto activated carbon," **4** 2018–2028 (2018). doi:10.15017/1960664.
- 5) K. Uddin, I.I. El-Sharkawy, T. Miyazaki, B.B. Saha, and S. Koyama, "Thermodynamic analysis of adsorption cooling cycle using ethanol-surface treated maxsorb iii pairs," *Evergreen*, **1** (1) 25–31 (2014). doi:10.5109/1440973.
- 6) F. Jerai, T. Miyazaki, B.B. Saha, and S. Koyama, "Overview of adsorption cooling system based on activated carbon - alcohol pair," *Evergreen*, **2** (1) 30–40 (2015). doi:10.5109/1500425.
- 7) M. Sultan, I.I. El-Sharkawy, T. Miyazaki, B.B. Saha, and S. Koyama, "Experimental study on carbon based adsorbents for greenhouse dehumidification," *Evergreen*, **1** (2) 5–11 (2014).
- 8) Y. Zheng, Q. Li, C. Yuan, Q. Tao, Y. Zhao, G. Zhang, J. Liu, and G. Qi, "Thermodynamic analysis of high-pressure methane adsorption on coal-based activated carbon," *Fuel*, **230** (May) 172–184 (2018). doi:10.1016/j.fuel.2018.05.056.
- 9) Y. Zheng, Q. Li, C. Yuan, Q. Tao, Y. Zhao, G. Zhang, and J. Liu, "Influence of temperature on adsorption selectivity: coal-based activated carbon for ch₄ enrichment from coal mine methane," *Powder Technol.*, **347** 42–49 (2019). doi:10.1016/j.powtec.2019.02.042.
- 10) S. Gao, L. Ge, T.E. Rufford, and Z. Zhu, "The preparation of activated carbon discs from tar pitch and coal powder for adsorption of co₂, ch₄ and n₂," *Microporous Mesoporous Mater.*, **238** 19–26 (2017). doi:10.1016/j.micromeso.2016.08.004.
- 11) J.F. González, S. Román, C.M. González-García, J.M. Valente Nabais, and A.L. Ortiz, "Porosity development in activated carbons prepared from walnut shells by carbon dioxide or steam activation," *Ind. Eng. Chem. Res.*, **48** (20) 9354–9354 (2009). doi:10.1021/ie9013293.
- 12) O. Ioannidou, and A. Zabaniotou, "Agricultural residues as precursors for activated carbon production-a review," *Renew. Sustain. Energy Rev.*, **11** (9) 1966–2005 (2007). doi:10.1016/j.rser.2006.03.013.
- 13) J. He, D. Zhang, M. Han, X. Liu, Y. Wang, Y. Li, X. Zhang, K. Wang, H. Feng, and Y. Wang, "One-step large-scale fabrication of nitrogen doped microporous carbon by self-activation of biomass for supercapacitors application," *J. Energy Storage*, **21** (November 2018) 94–104 (2019).

- doi:10.1016/j.est.2018.11.015.
- 14) T. Mahmood, R. Ali, A. Naeem, M. Hamayun, and M. Aslam, "Potential of used camellia sinensis leaves as precursor for activated carbon preparation by chemical activation with h3po4; optimization using response surface methodology," *Process Saf. Environ. Prot.*, **109**, 548–563 (2017). doi:10.1016/j.psep.2017.04.024.
- 15) J. Pallarés, A. González-Cencerrado, and I. Arauzo, "Production and characterization of activated carbon from barley straw by physical activation with carbon dioxide and steam," *Biomass and Bioenergy*, **115** (January) 64–73 (2018). doi:10.1016/j.biombioe.2018.04.015.
- 16) M. Olivares-Marín, C. Fernández-González, A. Macías-García, and V. Gómez-Serrano, "Preparation of activated carbon from cherry stones by physical activation in air. influence of the chemical carbonisation with h2so4," *J. Anal. Appl. Pyrolysis*, **94** 131–137 (2012). doi:10.1016/j.jaap.2011.11.019.
- 17) Suhas, P.J.M. Carrott, M.M.L. Ribeiro Carrott, R. Singh, L.P. Singh, and M. Chaudhary, "An innovative approach to develop microporous activated carbons in oxidising atmosphere," *J. Clean. Prod.*, **156**, 549–555 (2017). doi:10.1016/j.jclepro.2017.04.078.
- 18) U.S. Im, J. Kim, S.H. Lee, S. mi Lee, B.R. Lee, D.H. Peck, and D.H. Jung, "Preparation of activated carbon from needle coke via two-stage steam activation process," *Mater. Lett.*, **237** 22–25 (2019). doi:10.1016/j.matlet.2018.09.171.
- 19) G.M. Brito, D.F. Cipriano, M.Â. Schettino, A.G. Cunha, E.R.C. Coelho, and J.C. Checon Freitas, "One-step methodology for preparing physically activated biocarbons from agricultural biomass waste," *J. Environ. Chem. Eng.*, **7** (3) 103113 (2019). doi:10.1016/j.jece.2019.103113.
- 20) T. Horikawa, S. (Johnathan) Tan, D.D. Do, K.I. Sotowa, J.R. Alcántara-Avila, and D. Nicholson, "Temperature dependence of water adsorption on highly graphitized carbon black and highly ordered mesoporous carbon," *Carbon N. Y.*, **124** 271–280 (2017). doi:10.1016/j.carbon.2017.08.067.
- 21) A. Mamani, M.F. Sardella, M. Giménez, and C. Deiana, "Highly microporous carbons from olive tree pruning: optimization of chemical activation conditions," *J. Environ. Chem. Eng.*, **7** (1) 102830 (2019). doi:10.1016/j.jece.2018.102830.
- 22) Y.J. Heo, and S.J. Park, "A role of steam activation on co2 capture and separation of narrow microporous carbons produced from cellulose fibers," *Energy*, **91** 142–150 (2015). doi:10.1016/j.energy.2015.08.033.
- 23) J. Alcañiz-Monge, A. Linares-Solano, and B. Rand, "Mechanism of adsorption of water in carbon micropores as revealed by a study of activated carbon fibers," *J. Phys. Chem. B*, **106** (12) 3209–3216 (2002). doi:10.1021/jp014388b.
- 24) A. Malika, and A. Mohammed, "Kinetic and energy study of thermal degradation of biomass materials under oxidative atmosphere using tga , dta and dsc," *Sci. Technol.*, **1** (5) 74–78 (2014).
- 25) H.S. Choi, Y.S. Choi, and H.C. Park, "Fast pyrolysis characteristics of lignocellulosic biomass with varying reaction conditions," *Renew. Energy*, **42** 131–135 (2012). doi:10.1016/j.renene.2011.08.049.
- 26) M.S. Safdari, E. Amini, D.R. Weise, and T.H. Fletcher, "Heating rate and temperature effects on pyrolysis products from live wildland fuels," *Fuel*, **242** (January) 295–304 (2019). doi:10.1016/j.fuel.2019.01.040.
- 27) W.A. Wan Mahari, C.T. Chong, W.H. Lam, T.N.S.T. Anuar, N.L. Ma, M.D. Ibrahim, and S.S. Lam, "Microwave co-pyrolysis of waste polyolefins and waste cooking oil: influence of n2 atmosphere versus vacuum environment," *Energy Convers. Manag.*, **171** 1292–1301 (2018). doi:10.1016/j.enconman.2018.06.073.
- 28) D. Özçimen, and A. Ersoy-Meriçboyu, "A study on the carbonization of grapeseed and chestnut shell," *Fuel Process. Technol.*, **89** (11) 1041–1046 (2008). doi:10.1016/j.fuproc.2008.04.006.
- 29) K. Stafford, W. Sing, and J. Rouquerol, "Reporting physisorption data for gas / solid systems including catalysis * reporting physisorption data for gas / solid systems with special reference to the determination of surface area and porosity," *Pure Appl. Chem.*, **57** (January 1985) 603–619 (2016).
- 30) T. Horikawa, Y. Kitakaze, T. Sekida, J. Hayashi, and M. Katoh, "Characteristics and humidity control capacity of activated carbon from bamboo," *Bioresour. Technol.*, **101** (11) 3964–3969 (2010). doi:10.1016/j.biortech.2010.01.032.
- 31) A.W. Harding, N.J. Foley, P.R. Norman, D.C. Francis, and K.M. Thomas, "Diffusion barriers in the kinetics of water vapor adsorption/desorption on activated carbons," *Langmuir*, **14** (14) 3858–3864 (1998). doi:10.1021/la971317o.
- 32) E.A. Müller, L.F. Rull, L.F. Vega, and K.E. Gubbins, "Adsorption of water on activated carbons: a molecular simulation study," *J. Phys. Chem.*, **100** (4) 1189–1196 (1996). doi:10.1021/jp952233w.
- 33) X. Li, X. Chen, and Z. Li, "Adsorption equilibrium and desorption activation energy of water vapor on activated carbon modified by an oxidation and reduction treatment," *J. Chem. Eng. Data*, **55** (9) 3164–3169 (2010). doi:10.1021/je100024r.
- 34) M.H. Mahmood, M. Sultan, T. Miyazaki, and S. Koyama, "Desiccant air-conditioning system for storage of fruits and vegetables: pakistan preview," *Evergreen*, **3** (1) 12–17 (2016). doi:10.5109/1657381.